AN INTRODUCTORY DISCUSSION OF THE STRUCTURE OF SINGLE-WALLED CARBON NANOTUBES AND THE RELATION BETWEEN CARBON NANOTUBE STRUCTURE AND THEIR ELECTRONIC PROPERTIES

DIANA L. GOELLER

ABSTRACT. This paper introduces the carbon nanotube (CNT). After a brief overview of its history, the structure of a CNT is examined at length. The sensitivity of the CNT's electrical properties to its structural geometry is discussed, touching on the band gap properties of graphene and how these differ from those of CNTs. The discussion is rounded off with brief consideration of a developing application of CNTs, the field-effect transistor (CNTFET).

1. INTRODUCTION

Carbon fibers have long been known to be a strong, lightweight, and thermally and electrically conductive material, and have been studied and used in various industrial applications for over a century. Thomas Edison used carbon fibers in early prototypes of his electric light bulb. Following WWII, a military-inspired boom in carbon fiber research led to advancement in long strings of the strong, lightweight material. A desire for controlled synthesis of crystalline fibers began in the 1960s with a catalytic chemical vapor deposition (CVD) process, which occasionally resulted in very thin fibers, but an interest in these was not taken until the discovery of fullerenes by Kroto and Smalley in 1990. In August of 1991, M.S. Dresselhaus delivered a discussion of the theoretical existence of carbon fibers with diameters on the scale of fullerenes, and these were finally observed by Iijima in 1991. Since then, carbon nanotube (CNT) research has progressed very rapidly [11].

In 1993, Iijima obtained the first experimental evidence of single-walled carbon nanotubes via transmission electron microscopy (TEM) [9], and the structure and physical properties have since been studied in depth. The fundamentals of the structural and electrical discoveries are discussed below. Meanwhile, industrial engineers have explored the potential uses of single- and multi-walled carbon nanotubes for a wide variety of purposes. The short carbon-carbon sp^2-hybrid bonds are still coveted for their incredible strength and light weight, but current research suggests that their greatest impact in future technology will be in electronics. One important application of semi-conducting carbon nanotubes will be superficially discussed at the end of this paper, but the reader is encouraged to investigate further the current technological research in this field.

2. CNT Structure

A single-walled carbon nanotube (SWNT) is a seamless cylinder of carbon formed by a single layer of the honeycomb-structured graphene, capped by rounded fullerene-structured ends. Most are 0.7-10.0 nm in diameter [11] and have been synthesized to be several millimeters in length [7]. Due to this large aspect ratio of length to diameter, the effects of the fullerene end caps on the physical properties of CNTs may be disregarded, and so we only consider the structure of the effectively one-dimensional tubes themselves.

Interestingly, a huge variability in nanotube structure, including diameter, arises from the angle at which the axes of the honeycomb structure lie with respect to the axis of the tube. 1 depicts the three distinct types of nanotube structures. 1a and 1b show "armchair" and "zigzag" structures, respectively (the names derive from the shape of the cross-sectional ring, also depicted in 1. These structures are achiral, or symmorphic, meaning they contain mirror planes through the nanotube axis, unlike the nanotube depicted in 1c, which is chiral or non-symmorphic, and hence this structure is known as "chiral" [11].
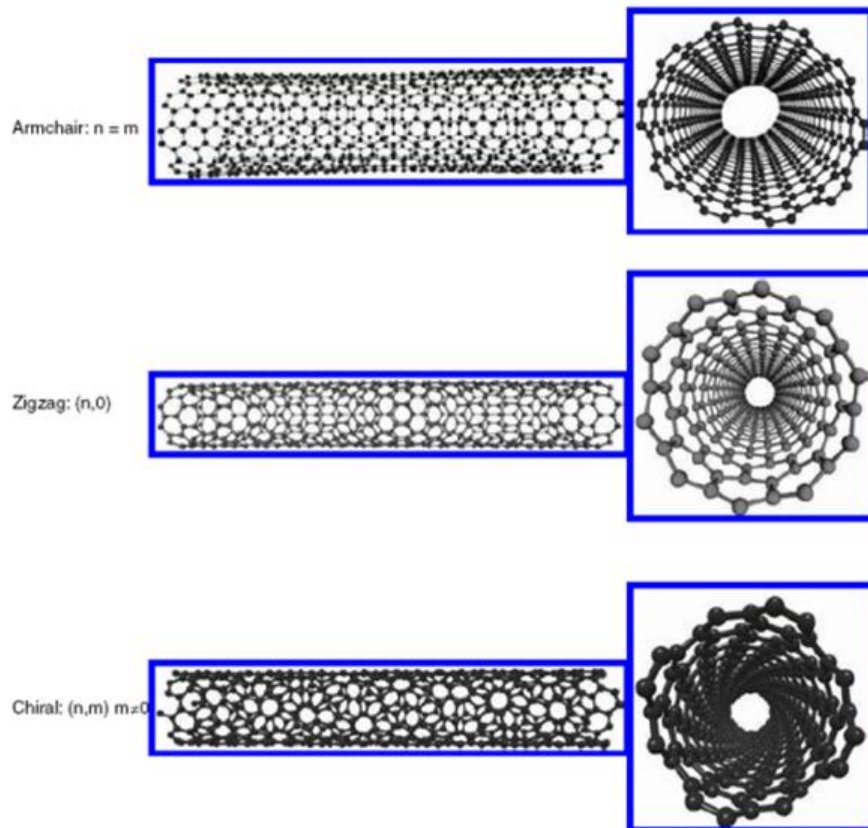

FIGURE 1. CNT structural types viewed longitudinally and in cross-section. 1a armchair. 1b zigzag. 1c chiral. From [7, p. 7].

The structure of a nanotube can be completely described mathematically in terms of three vectors: the chiral vector $\vec{C}_h$, the translation vector $\vec{T}$, and the symmetry vector $\vec{S}$.

2.1. The Chiral Vector $\vec{C}_h$.

The structure of a carbon nanotube is uniquely defined by the vector (OA in **??**) that lies perpendicular to the axis of the nanotube [11, p. 37]. Because this vector determines the chirality of the nanotube, it is termed the chiral vector $\vec{C}_h$, and it is defined in terms of the real space basis unit vectors $\hat{a}_1$ and $\hat{a}_2$ of the hexagonal lattice of graphene (shown in **??**):

$$\vec{C}_h = n\hat{a}_1 + m\hat{a}_2 \equiv (n, m) \quad (n, m \text{ integers}, \ 0 \le |m| \le n) \tag{1}$$

This vector defines an equator of the nanotube, such that when the graphene sheet depicted in **??** is rolled up to produce a nanotube, the ends of $\vec{C}_h$ will be superimposed; its length C_h is therefore the circumference of the nanotube. From this we can determine the diameter d_t of the nanotube:

$$d_t = \frac{C_h}{\pi} = \frac{\sqrt{\vec{C}_h \cdot \vec{C}_h}}{\pi} = \frac{a}{\pi}\sqrt{n^2 + nm + m^2} = \frac{\sqrt{3} \cdot a_{C-C}}{\pi} \cdot \sqrt{n^2 + nm + m^2} \tag{2}$$

in which a is the magnitude of the unit vectors $|\hat{a}_1| = |\hat{a}_2| = \sqrt{3} \cdot a_{C-C}$, and a_{C-C} is the carbon-carbon bond length (1.44Å in carbon nanotubes).
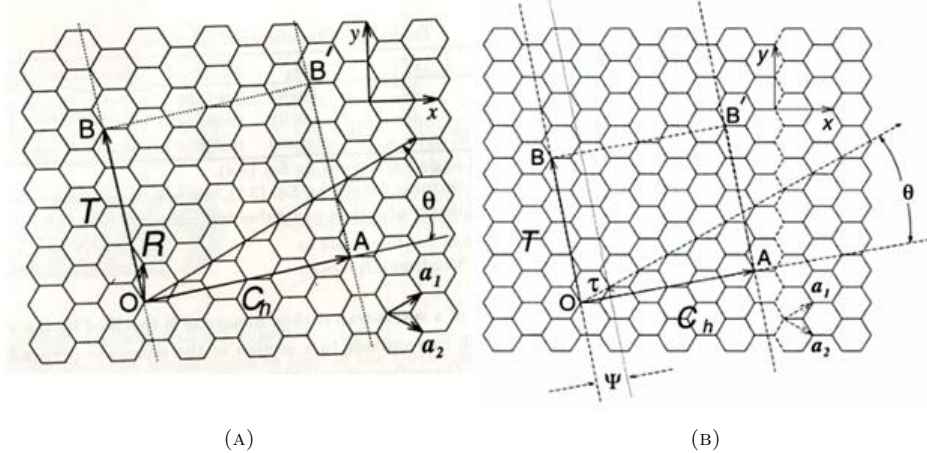

(A)   (B)

FIGURE 2. Schematic of "unrolled" CNT. The chiral vector $\vec{C}_h$ is the line segment OA. The translation vector $\vec{T}$ is the line segment OB, parallel to the nanotube axis and perpendicular to $\vec{C}_h$, the length of which is the circumference of the nanotube. Cartesian axes x and y are shown, as are the basis vectors $\hat{a}_1$ and $\hat{a}_2$ that define the unit cell for graphite. $\vec{C}_h$ and $\vec{T}$ define the unit cell of the CNT. The chiral angle θ measures the angle of $\vec{C}_h$ from a line parallel to $\hat{a}_1$. 2a shows the symmetry vector, $\vec{S}$ while 2b shows the rotation angle ψ and the translation distance τ that characterize $\vec{S}$, which maps every lattice point in the unit cell, outlined by rectangle $OAB'B$. 2a from [11, p. 38]. 2b from [4, p. 28].

For derivational purposes, it is useful to note that, because $\hat{a}_1$ and $\hat{a}_2$ are not perpendicular but rather at 60° to one another, the dot products that were implicitly calculated in (2) are, explicitly:

$$\hat{a}_1 \cdot \hat{a}_1 = \hat{a}_2 \cdot \hat{a}_2 = a^2 \cos\left(0°\right) = a^2 \tag{3a}$$

$$\hat{a}_1 \cdot \hat{a}_2 = a^2 \cos\left(60°\right) = \frac{a^2}{2}. \tag{3b}$$

The values of the integers (n, m) determine the chirality of the nanotube, which in turn regulates its physical properties. In the case of $n = m$, the chiral vector travels in the direction of the x-axis, shown in **??**. This results in the "armchair" structure shown in 1a. In the case where $n = 0$ or $m = 0$ (which are symmetrically equivalent), the chiral vector travels in the direction of $\hat{a}_1$ (or $\hat{a}_2$), resulting in the "zigzag" structure shown in 1b. Recall, these types are both achiral. Any other ordered pair (n, m) defines a chiral vector [4, 11].

2.1.1. *The Chiral Angle θ.* Oftentimes, the chirality of a nanotube is described by the angle θ that the chiral vector makes with the $\hat{a}_1$ unit vector. This angle, known as the chiral angle, can be defined by the dot-product relation between the angles:

$$\cos\theta = \frac{\vec{C}_h \cdot \hat{a}_1}{\left|\vec{C}_h\right|\left|\hat{a}_1\right|} = \frac{2n + m}{2\sqrt{n^2 + nm + m^2}}. \tag{4}$$

Similarly, taking the cross product of $\vec{C}_h$ and $\vec{a}_1$ gives us an equation for $\sin\theta$, from which we can derive the simpler expression

$$\tan\theta = \frac{\sin\theta}{\cos\theta} = \sqrt{3} \cdot \frac{n}{2m + n}. \tag{5}$$

We can check the validity of these equations by considering them in light of what we already know. In the case of a zigzag structure, for which $n = 0$, we conclude from (4) that $\theta = 0$, which is consistent with our definition of the chiral vector for a zigzag structure, parallel to $\hat{a}_1$. It is important to note that if $m = 0 \neq n$, (4) still shows that $\theta = 0$, but (5) gives $\theta = 60°$. This corresponds to the chiral vector aligning with $\hat{a}_2$ rather than $\hat{a}_1$, but because of the hexagonal symmetry of the CNT structure, this is ultimately equivalent. In fact, we could also define $\tan\theta$ as

$$\tan\theta = \sqrt{3} \cdot \frac{m}{2m + n} \tag{5'}$$

which yields $\theta = 0$ when $m = 0$ and $\theta = 60°$ when $n = 0$, but again, the two are symmetrically equivalent. We can therefore limit θ to $0 \leq \theta \leq 30°$, in which case θ is unambiguously 0 in the case where either n or m is 0.

Armchair nanotube structures, for which $n = m$, show the other extreme; by (4) and (5) (or (5')), we find that $\theta = 30°$, which is likewise consistent with our previous definition. All other nanotubes, i.e. chiral nanotubes, have $0 < \theta < 30°$ [4, 11].

2.2. **The Translation Vector $\vec{T}$.** Together, the chiral vector $\vec{C}_h$ and the translation vector $\vec{T}$ (OB in **??**) define the unit cell of a uniform carbon nanotube [7], and $\vec{T}$ is taken to be the unit vector of the one-dimensional structure [11, p. 39]. $\vec{T}$ is perpendicular to $\vec{C}_h$ and parallel to the nanotube axis, and its length T is defined as the shortest distance in that direction from the lattice point at the tail of $\vec{C}_h$ to

an equivalent lattice point. Mathematically, this can be expressed in terms of the unit vectors $\hat{a}_1$ and $\hat{a}_2$ of the honeycomb lattice as:

$$\vec{T} = t_1 \cdot \hat{a}_1 + t_2 \cdot \hat{a}_2 \equiv (t_1, t_2) \tag{6}$$

where $t_1, t_2 \in \mathbb{Z}$ are coprime, meaning $\gcd(t_1, t_2) = 1$. Then, using $\vec{C}_h \cdot \vec{T} = 0$ and equations (1), (3a), (3b), and (6), we can derive expressions for t_1 and t_2:

$$t_1 = \frac{2m + n}{d_R}, \qquad t_2 = \frac{2n + m}{d_R} \tag{7}$$

in which d_R is $\gcd(2m + n, 2n + m)$. If we introduce the parameter d as $\gcd(n, m)$, we can perhaps more quickly calculate d_R by noting the relation:

$$d_R = \begin{cases} d & \text{if } nm \text{ is not a multiple of } 3d \\ 3d & \text{if } nm \text{ is a multiple of } 3d. \end{cases} \tag{8}$$

Then, using (7), we can derive the magnitude of $\vec{T} = |\vec{T}| = T$ as given by:

$$T = |\vec{T}| = \sqrt{\vec{T} \cdot \vec{T}} = \frac{a}{d_R} \cdot \sqrt{3n^2 + 3nm + 3m^2} = \frac{\sqrt{3}}{d_R} \cdot \vec{C}_h \tag{9}$$

[4, 11].

2.2.1. *Size of the Unit Cell.* As noted above, the unit cell of a carbon nanotube is defined by the vectors $\vec{C}_h$ and $\vec{T}$. This unit cell is much larger that of the isostructural graphene, defined by the unit vectors $\hat{a}_1$ and $\hat{a}_2$. Because the unit cell of graphene is a single hexagon, the quotient of the areas of these unit cells defines the integer number N of hexagons in the unit cell of the nanotube:

$$N = \frac{|\vec{C}_h \times \vec{T}|}{|\hat{a}_1 \times \hat{a}_2|} = 2\frac{n^2 + nm + m^2}{d_R} = \frac{2C_h^2}{a^2 \cdot d_R}. \tag{10}$$

It is also useful to note that each hexagon "owns" two carbon atoms, so there are $2N$ carbon atoms in each unit cell of a nanotube [4, 11].

2.3. **The Symmetry Vector $\vec{S}$.** The symmetry vector $\vec{S}$ is used to generate the coordinates of all carbon atoms in the unit cell of a CNT from an initial carbon atom. The coordinates are described by site vectors, which are each an integer multiples of $\vec{S}$,

$$V_i \equiv i\vec{S} \qquad (i = 1, 2, \cdots, N). \tag{11}$$

Each site vector defines the coordinates of one carbon atom in a hexagon (the unit cell for graphene), from which the positions of the other carbon atoms belonging to that hexagon can be derived; the N site vectors defined by $\vec{S}$ correspond to symmetrically equivalent corners of the N carbon hexagons that make up the CNT unit cell. Like the chiral vector, the symmetry vector is defined by a pair of coprime integers, (p, q), that represent the coefficients of the basis vectors that define $\vec{S}$ for a particular nanotube:

$$\vec{S} = p\hat{a}_1 + q\hat{a}_2 \equiv (p, q). \tag{12}$$

Defining $\vec{S}$ to lie between the chiral and translation vectors in the plane of the graphene sheet, it is convenient to describe the symmetry vector in terms of its components parallel to each of these, as shown in **??** and 3. The component parallel to the chiral vector is proportional and parallel to $\vec{T} \times \vec{S}$, which is given by

$$\vec{T} \times \vec{S} = (t_1 q - t_2 p) \cdot (\hat{a}_1 \times \hat{a}_2) \tag{13}$$

where $t_1q - t_2p$ is an integer. We select p and q or $\vec{S}$ to form the smallest site vector $(i = 1)$ so that

$$t_1q - t_2p = 1 \tag{14}$$

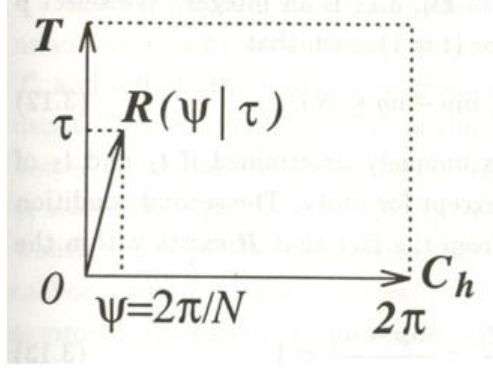which has a unique solution if $\gcd t_1, t_1 = 1$.

FIGURE 3. The projection of the symmetry vector $\vec{S}$ onto the chiral and translation vectors separates the rotational and translational components of the nanotube symmetry. The angle ψ and translation τ together define the space group symmetry inherent in the carbon nanotube uniquely defined by the chiral vector ordered pair (n, m). From [11, p. 41].

Combining equations (2), (9), and (10), we derive an important relation amongst the three fundamental unit cell vectors. By showing that

$$0 < \frac{\vec{S} \cdot \vec{T}}{T^2} = \frac{|C_h \times \vec{S}|}{C_h T} = \frac{mp - nq}{N} < 1 \tag{15}$$

we see that

$$0 < mp - nq \leq N. \tag{16}$$

Similarly combining equations (7) and (10), we find another necessary consequence arising from $\vec{S}$ residing within the unit cell:

$$0 < \frac{\vec{S} \cdot \vec{C_h}}{C_h^2} = \frac{|\vec{S} \times \vec{T}|}{C_h T} = \frac{t_1q - t_2p}{N} < 1 \tag{17}$$

From which we obtain the condition

$$0 < t_1q - t_2p < N. \tag{18}$$

But this is trivially satisfied by equation (14). In fact, in other definitions of the symmetry vector, $t_1q - t_2p$ is not necessarily 1, but it is always some integer Q defined on the interval $1 \leq Q \leq N$. Here we will define $Q = 1$ for simplicity.

To determine all N site location vectors defined in (11) of the nanotube unit cell, we multiply the smallest site vector $1 \cdot \vec{S}$ by each integer on the interval $[1, N]$. The coordinate in the circumferential direction is given by $i(t_1q - t_2p)$. We can check

that this defines N distinct sites in the CNT unit cell by noting that $N\vec{S} = |\vec{C}_h| = C_h$, which we obtain from combining equations (9) and (10):

$$\frac{N\vec{S}\cdot\vec{C}_h}{C_h} = \frac{N|\vec{S}\times\vec{T}|}{T} = \frac{2C_h^2}{d_R a^2}\cdot\frac{\sqrt{3}a^2}{2}\cdot\frac{d_R}{\sqrt{3}C_h} = C_h. \tag{19}$$

Therefore, (11) generates all N atom positions in a CNT unit cell.

Geometrically, the vector $\vec{S}$ can be broken into a rotation by an angle ψ about the nanotube axis, which is the component of $\vec{S}$ parallel to the chiral vector $\vec{C}_h$, scaled by a factor of C_h/d_t, and a translation τ along the nanotube axis, which is the component of $\vec{S}$ parallel to the translational vector $\vec{T}$ (see 3). Thus $\vec{S}$ contains all the information about the space group symmetry of an arbitrary chiral CNT, where the symmetry operation is denoted $\vec{S} = (\psi|\tau)$. This operator acting on an atom at a defined origin $(0,0)$ produces the previously defined integers p and q. Each of the other $N-1$ hexagons in the unit cell are denoted by the symmetry operations $(\psi|\tau)^2, \cdots, (\psi|\tau)^N$, where $(\psi|\tau)^N$ is the identity operation which maps point O onto point C in 4.
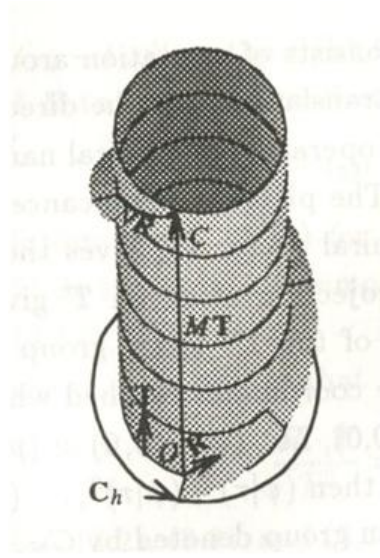

FIGURE 4. The symmetry vector $\vec{S}$ produces the coordinates of every hexagon in the unit cell of an arbitrary chiral CNT from a given origin point O by multiplying the smallest site vector, defined to be $\vec{S}$, by the set of integers on the interval from 1 to N, where N is the number of hexagons in the unit cell of the CNT. As the symmetry vector spirals along the CNT axis, every hexagon has a different projection onto the chiral vector Ch until $\vec{S}$ has defined all N sites in the CNT unit cell, at which point the vector $N\vec{S}$ will define a point C which is symmetrically identical to the origin point O. From [11, p. 44].

For exact expressions for the rotation angle ψ and the translation distance τ for an arbitrary chiral CNT defined by the chiral vector integers (n, m), we take the

indicated vector products and use equations (9), (10), and (14) to obtain

$$\psi = \frac{|\vec{T} \times \vec{S}|}{T} \cdot \frac{2\pi}{C_h} = \frac{d_R(t_1 q - t_2 p)}{\sqrt{3}C_h} \cdot \frac{\sqrt{3}a^2}{2} = \frac{2\pi}{N} \tag{20}$$

Table 1. Parameters of carbon nanotubes

Symbol	Name	Formula	Value
$a_{C\text{-}C}$	carbon-carbon distance		1.421 Å (graphite)
a	length of unit vector	$\sqrt{3}a_{C\text{-}C}$	2.46 Å
$\mathbf{a}_1, \mathbf{a}_2$	unit vectors	$\left(\frac{\sqrt{3}}{2}, \frac{1}{2}\right)a, \left(\frac{\sqrt{3}}{2}, -\frac{1}{2}\right)a$	in (x, y) coordinates
$\mathbf{b}_1, \mathbf{b}_2$	reciprocal lattice vectors	$\left(\frac{1}{\sqrt{3}}, 1\right)\frac{2\pi}{a}, \left(\frac{1}{\sqrt{3}}, -1\right)\frac{2\pi}{a}$	in (x, y) coordinates
$\mathbf{C}_h$	chiral vector	$\mathbf{C}_h = n\mathbf{a}_1 + m\mathbf{a}_2 \equiv (n, m)$	n, m: integers
L	circumference of nanotube	$L = |\mathbf{C}_h| = a\sqrt{n^2 + m^2 + nm}$	$0 \le |m| \le n$
d_t	diameter of nanotube	$d_t = \frac{L}{\pi} = \frac{\sqrt{n^2 + m^2 + nm}}{\pi}a$	
θ	chiral angle	$\sin\theta = \frac{\sqrt{3}m}{2\sqrt{n^2 + m^2 + nm}}$	$0 \le |\theta| \le 30°$
		$\cos\theta = \frac{2n + m}{2\sqrt{n^2 + m^2 + nm}}$	
		$\tan\theta = \frac{\sqrt{3}m}{2n + m}$	
d	the highest common divisor of (n, m)		
d_R	the highest common divisor of $(2n + m, 2m + n)$	$d_R = \begin{cases} d & \text{if } n - m \text{ not a multiple of } 3d \\ 3d & \text{if } n - m \text{ a multiple of } 3d. \end{cases}$	
$\mathbf{T}$	translational vector of 1D unit cell	$\mathbf{T} = t_1\mathbf{a}_1 + t_2\mathbf{a}_2 \equiv (t_1, t_2)$	t_1, t_2: integers
		$t_1 = \frac{2m + n}{d_R}$	
		$t_2 = -\frac{2n + m}{d_R}$	
T	length of $\mathbf{T}$	$T = \frac{\sqrt{3}L}{d_R}$	
N	number of hexagons per 1D unit cell	$N = \frac{2(n^2 + m^2 + nm)}{d_R}$	$2N \equiv n_C/\text{unit cell}$
$\mathbf{R}$	symmetry vector‡	$\mathbf{R} = p\mathbf{a}_1 + q\mathbf{a}_2 \equiv (p, q)$	p, q: integers†
		$d = mp - nq, 0 \le p \le n/d, 0 \le q \le m/d$	
M	number of 2π revolutions	$M = [(2n + m)p + (2m + n)q]/d_R$	M: integer
		$N\mathbf{R} = M\mathbf{C}_h + d\mathbf{T}$	
R	basic symmetry operation‡	$R = (\psi|\tau)$	
ψ	rotation operation	$\psi = 2\pi\frac{M}{N}, \left(\chi = \frac{\psi L}{2\pi}\right)$	ψ: radians
τ	translation operation	$\tau = \frac{d\mathbf{T}}{N}$	τ, χ: length

†(p, q) are uniquely determined by $d = mp - nq$, subject to conditions stated in table, except for zigzag tubes for which $\mathbf{C}_h = (n, 0)$, and we define $p = 1, q = -1$, which gives $M = 1$.
‡$\mathbf{R}$ and R refer to the same symmetry operation.

Table 1. Parameters of carbon nanotubes. From [4, p. 29].

and

$$\tau = \frac{|\vec{S} \times \vec{C_h}|}{C_h} = \frac{(mp - nq)|\hat{a_1} \times \hat{a_2}|}{C_h} = \frac{(mp - nq)T}{N} \tag{21}$$

[4, 11]. A summary of these fundamental relations of the structure of CNTs is given in Table 1 (taken from [4, p. 29]).

2.4. **A Note on Multi-Walled Carbon Nanotubes (MWNTs).** So far we have discussed the structure of single-walled carbon nanotubes (SWNTs), which can be thought of as a single layer of graphene rolled into a seamless cylinder at some angle θ, but the existence of SWNTs was not confirmed until 1993 [9], and today they cannot be synthesized without metal catalysts [10]. Iijima first observed multi-walled nanotubes (MWNTs), of 2-20 layers, via TEM in 1991 (see 5, from [7, p. 5]) [8]. MWNTs are coaxial SWNTs, with inter-layer distance similar to the inter-sheet distance in graphite (3.44Å) within some tolerance $\delta \sim 0.25$Å [3]. Their physical properties are somewhat different from those of SWNT, and they are also the topic of much of modern research, not least because they are cheaper and simpler to produce in bulk. However, these studies and applications are beyond the scope of this paper.
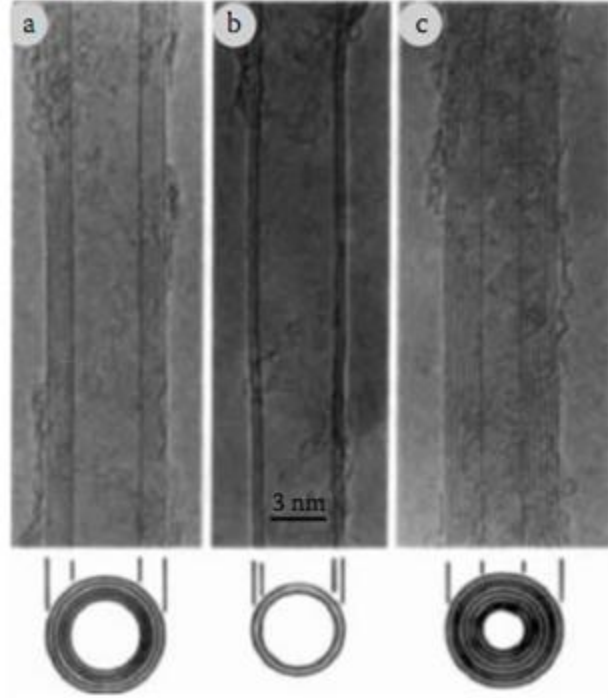

FIGURE 5. Multi-walled carbon nanotubes (MWCNTs) as seen through a transmission-electron microscope (TEM) by Sumio Iijima in 1991. 5a shows five concentric nanotubes, 5b shows two concentric nanotubes, and 5c shows seven concentric nanotubes. From [8, p. 56].

3. Quantum Mechanics of CNTs

To understand the intimate connection between the geometric structure of a CNT and its electronic properties, we now investigate in less detail the fundamental concepts of quantum mechanics that apply to the electric properties of CNTs. These include the concepts of reciprocal or k-space, the Brillouin zone, Fermi energy, and the basic concepts of Band Gap Theory.

3.1. **Reciprocal Space and Brillouin Zones.** Every periodic structure can be defined by either of two lattices [13]. The real space lattice, defined by the basis vectors $\hat{a_1}$, $\hat{a_2}$, and $\hat{a_3}$, is the more obvious of the two, and maps the periodicity of the real structure. In real space, these vectors define the unit cell of graphite. In two dimensions, $\hat{a_1}$ and $\hat{a_2}$ define the unit cell of graphene, as seen above, and the unit cell of a carbon nanotube is the rectangle defined by the chiral vector $\vec{C}_h$ and the translation vector $\vec{T}$, shown in **??** as $OAB'B$, and defined in terms of the real space unit vectors by equations (1) and (6), respectively. The electronic properties of the CNT, however, depend on the band gap structure of the lattice, which varies periodically according to the reciprocal lattice, which exists in what is known as reciprocal space.

Superficially, a reciprocal lattice is a different way to represent the geometry of the real lattice. Two-dimensional planes of atoms are represented by their one-dimensional normal vector, and the magnitude of this vector is proportional to the reciprocal of the distance between these planes of atoms [2]. Mathematically, this space has far greater consequences, which allow for complicated calculations, only a few of which will be touched on here.

Mathematically, a reciprocal lattice is defined by the set of all reciprocal lattice vectors K that satisfy Bloch's Theorem and the Schrödinger Equation, which can be simplified to the condition

$$e^{2\pi i \vec{K} \cdot \vec{R}} = 1 \qquad \text{(crystallographer's definition)} \tag{22}$$

in which $\vec{K}$ is a linear combination of the reciprocal basis vectors

$$\vec{K} = h\hat{b_1} + k\hat{b_2} + \ell\hat{b_3} \tag{23}$$

and $\vec{R}$ is called a real lattice vector, and is a linear combination of the real space basis vectors

$$\vec{R} = h\hat{a_1} + k\hat{a_2} + \ell\hat{a_3} \tag{24}$$

in which h, k, and ℓ are all integers. The reciprocal basis vectors are all defined in terms of the real basis vectors, according to the matrix transformation

$$[\hat{b_1}\hat{b_2}\hat{b_3}]^T = [\hat{a_1}\hat{a_2}\hat{a_3}]^{-1}. \tag{25}$$

By this definition, the reciprocal basis vector $\hat{b_1}$ (between two nearest lattice points; see **??**) has the reciprocal magnitude of real basis vector $\hat{a_1}$, and lies in the direction of $\hat{a_2} \times \hat{a_3}$, and so on for the other basis vectors [2].

Reciprocal space allows for direct comparison between the wave vector $\vec{k}$ of any given particle in the lattice, or of a charge carrier (electron) moving through the lattice, and an arbitrary reciprocal lattice vector $\vec{K}$. Because it is defined by the reciprocal lattice vectors denoted by the letter K, reciprocal space is also known as "k-space." In a graphene sheet and correspondingly in CNTs, in which the structure is only two-dimensional, only the first two basis vectors are important.
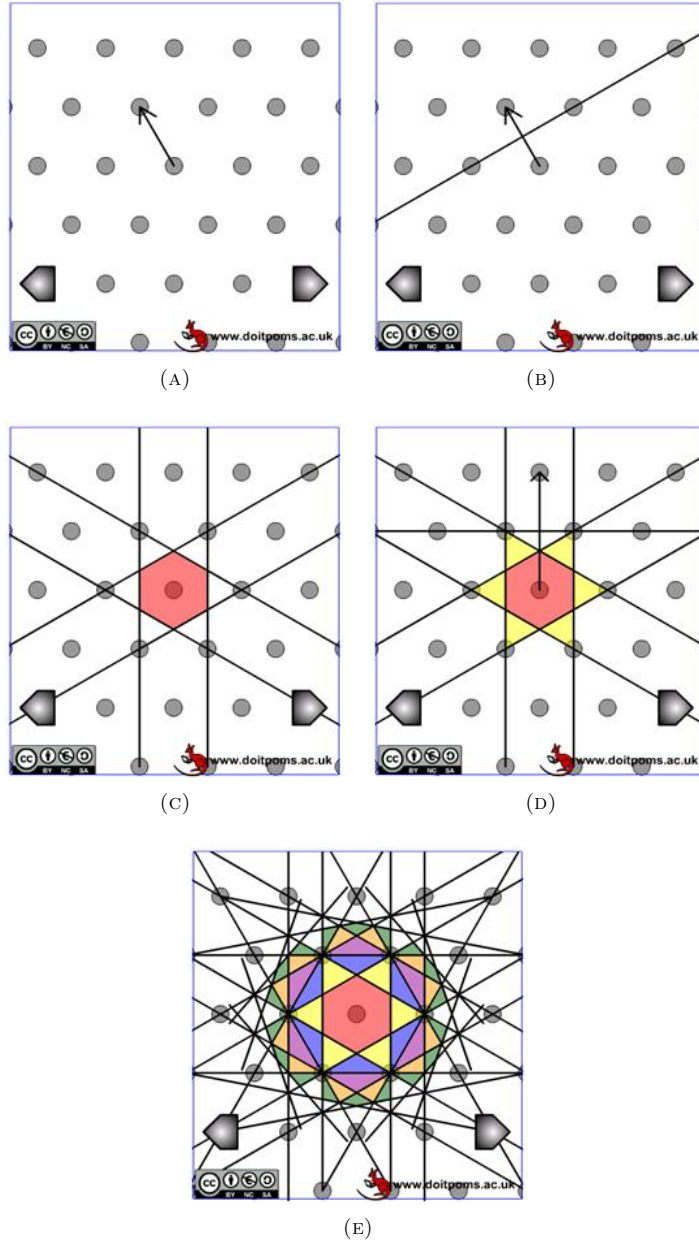
(A)

(B)

(C)

(D)

(E)

FIGURE 6. Brillouin Zones for an hexagonal reciprocal lattice. 6a From an arbitrary origin, draw a reciprocal lattice vector between two nearest points. 6b Construct the perpendicular bisector of this vector. This is a Bragg plane. 6c Repeat following the 6-fold symmetry. The first Brillouin zone is shaded red. 6d The same procedure can be used to find higher-order Brillouin zones. 6e The first six Brillouin zones.

Reciprocal space is also called Fourier space, because the mathematical transition from one to the other is a Fourier transform, which is also the relation between distance and momentum by way of the Hamiltonian operator. Because of this, the physical representation of distance and momentum is switched in reciprocal space, and the magnitude of a wave vector is directly proportional to the momentum of the particle associated with that wave vector. For this reason, reciprocal space is also called momentum space.

The Brillouin zone or the first Brillouin zone is the primitive cell of the reciprocal lattice. In two dimensions, its boundaries are defined by the perpendicular bisectors of the reciprocal lattice vectors from an arbitrary origin point to its nearest neighbors (6a-6c). Note that these boundaries are Bragg planes of waves generated by each particle, which may be represented by a different wave vector $\vec{k}$. Higher-order Brillouin Zones are found by the same method, and defined so that there are $N - 1$ Bragg planes between the origin point and the N-th Brillouin zone (6d-6e), but the electrical properties of the periodic structure depend only on the energies in the first Brillouin zone, so we will not consider the higher-order zones [13].
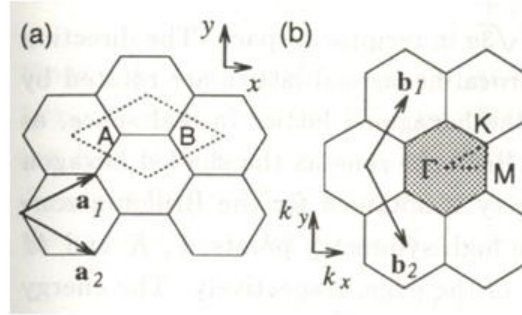

FIGURE 7. The primitive unit cells of graphene in 7a real space and 7b reciprocal space, also known as the Brillouin zone. The primitive basis vectors are shown for each case. The high-symmetry points of the reciprocal unit cell are also shown in b): Γ, M, and K. From [11, p. 25].

For most structures, Brillouin zones are three-dimensional, but because the structure of SWCNTs is geometrically nearly identical to that of a single graphene sheet, the first Brillouin zone is a simple, two-dimensional hexagon, as shown above. The center of the first Brillouin zone is denoted by Γ. In a 2D hexagonal cell, M denotes the center of a side, and K denotes a corner of the primitive Brillouin zone (7b). Because each cell owns two carbon atoms, these two points are sometimes differentiated as K and K', but because of the symmetry of the hexagonal Bravais lattice, these have the same quantum, and therefore electronic, properties. Notice that the reciprocal lattice for the graphene hexagonal real lattice is also hexagonal, but the real lattice points correspond to the Γ points in the reciprocal lattice, farthest from any of the reciprocal lattice points. In general, the Brillouin zone is not the same shape as the primitive cell of the real lattice.

3.2. **Fermi Energy and Band Gap Theory.** The sensitivity of the electronic properties of a CNT to its geometry is best explained by what is known as a band-folding picture. A wave vector $\vec{k}$ is a function of the energy of the particle associated with it; in momentum space, its magnitude is directly proportional to that of the momentum of the particle. Because of the translational symmetry of the lattice, the energy of the particles is also periodic. The periodicity is the reciprocal lattice vector, $\vec{K}$, meaning that all the symmetry of the periodic energy is contained within the first Brillouin zone. For a given wave vector and its associated potential, the Schrödinger equation gives two solutions for the particle energy, one associated with the bonding or valence orbitals (indicated by π in 8a) and one associated with the anti-bonding or conduction orbitals (indicated by π^* in 8a). These solutions are called bands, and they show the energy dispersion around the lattice.

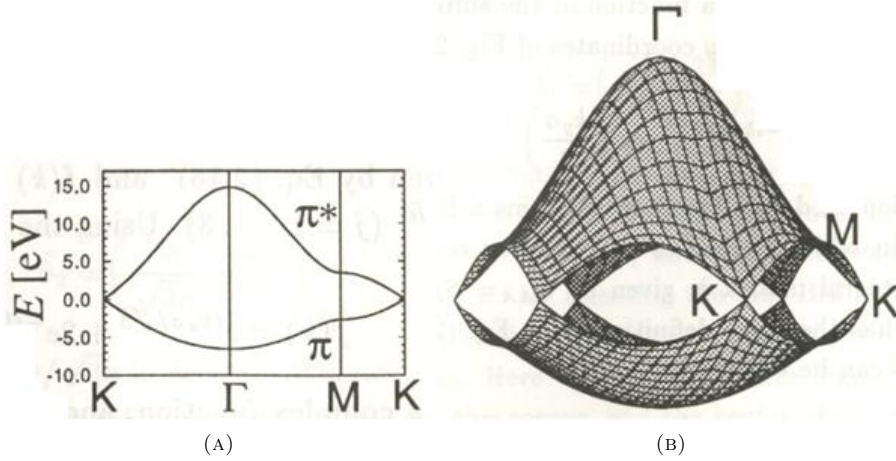(A)   (B)

FIGURE 8. Band structure of graphene. 8a shows the plot of electric potential along the high-symmetry triangle outlined in 7b. The energies are different for the bonding (valence) and anti-bonding (conduction) bands, indicated respectively by π and π^*. Notice that the energy bands are degenerate at the K point. 8b shows a three-dimensional extrapolation of the plotted data in 8a, labelling the important points of the Brillouin zone as in 7b.

Mathematically, it is difficult to solve for the energy dispersion relations for all values of $\vec{k}$, so only the directions of high symmetry within the Brillouin zone are considered. In graphene, this is the triangle formed by the points Γ, M, and K, as shown in 7b. The resulting qualitative potential plot is shown in 8a, and the extrapolated three-dimensional image, showing the energy dispersion relations over the whole first Brillouin zone, is shown in 8b. This is known as the band structure for the lattice [11].

The bonding and anti-bonding bands are separated at each $\vec{k}$ by some finite energy, represented along the vertical axis in the band structure models in 8a and 8b. In some cases, along the high-symmetry directions of the Brillouin zone, this energy difference might be zero, in which case the energy bands are said to be

degenerate. In graphene, the energy states are degenerate at all of the K and K' points in the lattice, and the energy here is the Fermi level [11]. This is the energy state that an arbitrary electron has a 50% chance of occupying at any given time. The degeneracy allows electrons to move freely between bands, which corresponds in real space to moving freely through the lattice. This explains why graphite is a good conductor. If the energy bands are not degenerate for any $\vec{k}$ in the band structure, there is said to be a (complete) band gap, which inhibits electrons from moving about the structure. If the band gap is relatively small, electrons are only somewhat inhibited, and the result is a semi-conductor [10]. As we will soon see, the electronic properties of CNTs are not identical to those of the unrolled graphene sheet. Rather, they depend on the ordered pair of integers (n, m) that define the Chiral vector, $\vec{C}_h$.

4. Electrical Properties of CNTs

4.1. **Metallic and Semiconducting CNTs.** In a carbon nanotube, the component of the wave vector $\vec{k}$ in the direction of the chiral vector $\vec{C}_h$ is denoted by $\vec{k}_C$, and is constrained by the cylindrical nature of the nanotube by the condition

$$\vec{k}_C \cdot \vec{C}_h = 2\pi j \qquad j \in \mathbb{Z}. \tag{26}$$

Therefore, the allowed wave vectors are quantized, and dependent on the diameter d_t of the nanotube, which is in turn dependent on the helicity

$$\vec{C}_h = \pi d_t. \tag{27}$$

This quantization leads to the different electric properties of CNTs of different diameters, as explained below. Meanwhile, the component of the wave vector $\vec{k}$ in the direction of the tube axis, parallel to the translation vector $\vec{T}$, denoted by $\vec{k}_T$, is continuous.

If (and only if) the K and K' points of the Brillouin zone lie on wave vectors allowed by the quantization constraint outlined above, the nanotube is metallic. As it happens, this occurs only for armchair nanotubes, when $n = m$. Otherwise, a band gap exists between the bonding and anti-bonding orbitals for all allowed wave vectors, and the nanotube is a semiconductor (the degree of conductivity depends on the size of the band gap, but this is never so wide as to be considered an insulator). However, in the special case where $n - m = 3j$, where j is an integer, the band gap between the valence and conduction bands is so small that, at room temperature, the nanotube is effectively metallic. These nanotubes are sometimes distinguished from zero gap and large gap semiconductors by the term "tiny gap" semiconductors (9) [10].

4.2. **Electrical Transport in CNTs.** Carbon nanotubes are characterized by long cylinders of tightly-bonded carbon atoms. This cylindrical nature makes perfect, i.e. defect-free, CNTs effectively one-dimensional, for all physical purposes. The smooth walls of carbon atoms connected by short and strong covalent bonds eliminate electron scattering in all directions except forward and backward along the tube, which does not greatly hinder electrical transport. Another common source of resistance in most electrical conduction is lattice vibration, but this is again minimized in the unique CNT structure by the very tight carbon-carbon bonds [1].
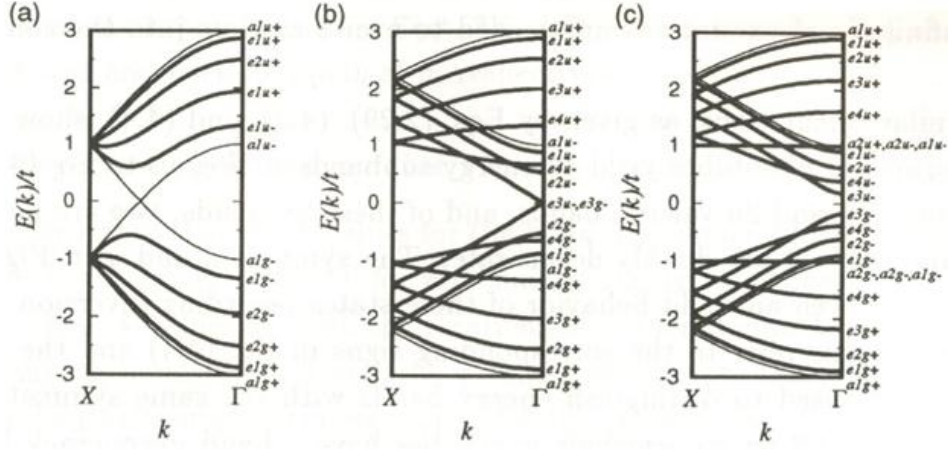
FIGURE 9. Band gaps in CNTs at K points in the Brillouin zone. 9a depicts an armchair CNT, which is metallic, as evidenced by the strong overlap in the lower bands of the valence and conduction orbitals. 9b depicts a tiny-gap semiconducting CNT, which is effectively a metallic CNT under certain conditions, including at room temperature. 9c depicts a true semiconducting CNT, with a small but complete band gap at the K point. From [11, p. 63].

The only sources of resistance in electron transport via CNTs, then, occur at the ends of the channels, where the one-dimensional CNTs connect to the three-dimensional metallic electrodes. However, because of the same circumferential quantization mentioned above, there are a small number of discrete energy states or modes that overlap with the continuous energy states of the electrodes. Because only energy states that overlap from the nanotube to the electrodes on either side can transport electrons, this leads to a quantized contact resistance, designated by R_C. The magnitude of the resistance is a function of the number of modes M in the CNT that have energies lying between the Fermi energies of the electrodes

$$R_C = \frac{h}{2e^2 M}. \tag{28}$$

in which h is Plank's constant and e is the fundamental electric charge. For a metallic (armchair) CNT, $M = 2$, so that $R_C = h/4e^2 = 6.45 k\Omega$ [1].

There are many other possible sources of resistance in CNT electronics, but when these are minimized so that the only resistance is this quantum resistance, electron transport in a CNT is said to be ballistic, meaning that no carrier scattering or energy dissipation takes place within the CNT [1]. This was once merely a theoretical concept, but since more work has been done with CNTs, researchers have started talking about this property of CNTs and the potential consequences in future applications. CNTs can only behave as ballistic conductors over a certain length, which depends on their structural perfection, the temperature, and the strength of the driving electric field, but these do not greatly hinder the importance of CNTs in future applications; ballistic transport can be achieved for lengths typical of and smaller than modern electronic devices (less than or equal to 100 nm), and even in

much longer sections, transport in CNTs can be as much as 1000 times higher than in bulk silicon [1].

Understanding some of the basic significance of CNTs in electronics, we now briefly turn our attention to one particular application of semi-conducting CNTs that shows high promise in the coming decades: the carbon nanotube field-effect transistor (CNTFET or CNFET).

5. The Future of Electronics: CNT Field-Effect Transistors

5.1. **Current Research.** Flow of electricity in a semiconductor requires either an external source of energy, such as heat or light absorption, to move the charge carriers over the energy band gap, or else a modulation of the gap that allows the electrons to freely cross it. In most modern electronics, an external electric field acts as a switch on the gap to allow electrons to pass (the ON position) or not (the OFF position). This modulating electronic field is known as the field-effect transistor (FET). Generally, a semiconducting channel connects two electrodes known as the source and the drain. Between these is a third electrode called a gate, and these three are all separated by some insulating film. An electric field applied at the gate with respect to the source will alter the conductance of the semiconducting channel, either allowing charge carriers (either electrons, carrying negative charge, or the absence of electrons known as a hole carrying positive charge and moving in the opposite direction) to flow freely in the material, or to inhibit their travel entirely, depending on its direction [1].

Currently, the standard FET is made from silicon and silicon dioxide, and is known as a metal-oxide semiconductor field-effect transistor (MOSFET). Casual observation, now know as Moore's Law, describes how the size of these electronics have halved approximately every two years for decades, but current technology now approaches the theoretical, minimum limits of this scaling. This has inspired widespread technological research for yet smaller, faster, and more efficient alternatives [1].

In 1998, Tans, et. al. produced a SWCNT FET that could operate at room temperature, and this is so far the only device to meet this important criteria for practical implementation [12]. Researchers have experimented with different types and styles of gate construction, and so far found that the "wrap-around" gate is most efficient, as shown in 10. In this configuration, especially because of the CNT's small diameter, the gate has maximum ability to regulate the potential of the channel. This strong so-called coupling between the gate and the channel allows the devices to be made even smaller (shorter) without incurring what are known as 'short-channel effects,' an infamous phenomenon resulting in loss of control of the device by the gate field [1].

Research in this field is still young but very extensive. Studies have established many advantages of CNTFETs over MOSFETs, including much higher current densities [5], much lower capacitance and somewhat lower operating voltage [1], roughly three times the on-current per unit width, compatibility with high-κ (more efficient) gate dielectrics, and double the carrier velocity [6]. They are also compatible with our current silicon technology, and can be scaled even smaller, and therefore faster, than silicon-based devices [5].
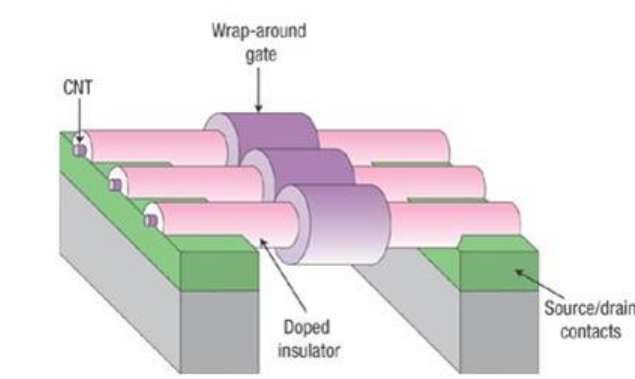
FIGURE 10. Wrap-around style CNTFET. The contact around the whole circumference of the CNT results in much greater efficiency than other styles of CNTFET connections. From [1, p. 607].

5.2. **Technological Limitations and Future Research.** Currently, the greatest limitation to CNT-based electronics is cost, which is dependent on researchers' ability to grow bulk wafers of structurally perfect CNTs, though recent advancements in chemical vapor deposition (CVD) technology may reduce this cost dramatically in the near future [5].

Future CNT-based transistors will likely operate at speeds on the scale of THz, and offer the potential for logic devices and cheaper and simpler self-assembly based fabrication. CNT-based transistors are already being used as biosensors. CNT-based light sources and detectors may lead to intra-chip optical communications, and individual molecule-level spectroscopy. The ballistic conduction of metallic CNTs may eventually lead to the development of single-component electronics, in which both the active devices and the connections between them are all based on the molecule carbon [1]. This is not even to mention the many other creative and useful applications of CNTs that scientists and engineers have thought up and are developing even now. These developments will define our technology in the decades, for decades, to come.

6. CONCLUSION

This paper introduced the concept of a carbon nanotube, initially in terms of its structure, and then in terms of its unique electronic properties. The physical construction of CNTs was thoroughly explained in terms of the chiral, translation, and symmetry vectors. The electronic properties of a CNT follow from its structure, which can be defined exactly and uniquely by either the ordered pair of integers (n, m) that define the chiral vector or the angle of rotation and distance of translation $(\psi|\tau)$ that define the symmetry vector. CNTs are divided into three types, based on their symmetry: armchair, zigzag, and chiral.

To better understand how the electronic properties of a CNT are described, background is provided on the concepts of reciprocal space and a reciprocal lattice. The first Brillouin zone is the primitive cell in a reciprocal lattice, and this is the smallest unit of translational symmetry within the energy band structure of a lattice. Because a CNT is geometrically similar to a rolled-up sheet of graphene,

the band structures are similar for graphene and for a CNT, but the helicity of the CNT affects its conductivity, and an arbitrary CNT can range almost continuously from metallic to semi-conducting, though only three types are ever differentiated: metallic CNTs consist only of the armchair structures, and the rest are either tiny-gap semiconductors, which are effectively metallic at room temperature, or small-gap, true semiconductors. Band gaps in a graphitic structure are never large enough to designate an insulator.

Though CNTs have many highly valuable characteristics, these and other highly valuable electric properties have inspired thousands of scientists and engineers around the globe to create the next generation of electronic devices, that will be smaller, faster, and lighter than the best silicon-based technology now or ever. One of the most important of these applications is the field-effect transistor, which is the basis of most modern microelectronics. If modern silicon-based MOTFETs are effectively replaced with CNTFETs, the technological advances that will follow are too numerous to list and almost too incredible to imagine. With the rapid advancement of this technology since CNTs were first discovered less than twenty years ago, it seems only a matter of time before this imagining becomes reality.

References

[1] Phaedon Avouris, Zhihong Chen, and Vasili Perebeinos. Carbon-based electronics. *Nature Nanotechnology*, 2:605–615, 2007.

[2] Leonid V. Azaroff. Reciprocal-lattice concept. In *Elements of x-ray crystallography*, pages 136–154. McGraw-Hill, Inc., New York, 1968.

[3] M. Damnjanović, I. Miločesić, E. Dobardžić, T. Vuković, and B. Nikolić. Symmetry based fundamentals of carbon nanotubes. In S. V. Rotkin and S. Subramoney, editors, *Applied physics of carbon nanotubes: fundamentals of theory, optics, and transport devices*, pages 41–88. Springer-Verlag, Berlin Heidelberg, 2005.

[4] M. S. Dresselhaus, G. Dresselhaus, and R. Saito. Physics of carbon nanotubes. In Morinubo Endo, Sumio Iijima, and Mildred S. Dresselhaus, editors, *Carbon nanotubes*, pages 27–35. Elsevier Science, Inc., 1994.

[5] Marcus Freitag. Carbon nanotube electronics and devices. In Michael J. O'Connell, editor, *Carbon nanotubes: properties and applications*, pages 83–117. 2006.

[6] Jing Guo, Supriyo Datta, and Mark Lundstrom. Assessment of silicon mos and carbon nanotube fet performance limits using a general theory of ballistic transistors. In *International Electron Devices Meetings (IEDM)*, page 711, 2002.

[7] Frank Henrich, Cadence Chan, Valerie Moore, Marco Rolandi, and Mike O'Connell. The element carbon. In Michael J. O'Connell, editor, *Carbon nanotubes: properties and applications*, pages 1–18. 2006.

[8] Sumio Iijima. Helical tubules of graphitic carbon. *Nature (London)*, 354:56–58, 1991.

[9] Sumio Iijima and Toshinari Ichihashi. Single-shell carbon nanotubes of 1-nm diameter. *Nature (London)*, 363:603–605, 1993.

[10] Steven G. Louie. Electronic properties, junctions and defects of carbon nanotubes. In M. S. Dresselhaus, G. Dresselhaus, and Ph. Avouris, editors, *Carbon*

nanotubes: synthesis, structure, properties and applications, pages 113–144. Springer-Verlag, Berlin Heidelberg, 2001.

[11] R. Saito, G. Dresselhaus, and M.S. Dresselhaus. *Physical properties of carbon nanotubes*. Imperial College Press, 1998.

[12] Sander J. Tans, Alwin R. M. Verschueren, and Cees Dekker. Room-temperature transistor based on single carbon nanotube. *Nature (London)*, 393:49–52, 1998.

[13] University of Cambridge. Brillouin zone DoITPoMS Learning Package. 2008. Available from `http://www.doitpoms.ac.uk/tlplib/brillouin_zones/`